AD_____

Award Number: DAMD17-00-C-0031

TITLE: Modeling for Military Operational Medicine Scientific and Technical Objectives

PRINCIPAL INVESTIGATOR: James H. Stuhmiller, Ph.D.
Weixin Shen, Ph.D.
Eugene Niu, Ph.D.
Adam Fournier

CONTRACTING ORGANIZATION: Jaycor
San Diego, California 92121-1190

REPORT DATE: September 2004

TYPE OF REPORT: Annual

PREPARED FOR: U.S. Army Medical Research and Materiel Command
Fort Detrick, Maryland 21702-5012

REPORT DOCUMENTATION PAGE

Form Approved
OMB No. 074-0188

1. AGENCY USE ONLY (Leave blank)	2. REPORT DATE	3. REPORT TYPE AND DATES COVERED
	September 2004	Annual (7 Aug 2003 - 6 Aug 2004)

4. TITLE AND SUBTITLE
Modeling for Military Operational Medicine Scientific and Technical Objectives

5. FUNDING NUMBERS
DAMD17-00-C-0031

6. AUTHOR(S)
James H. Stuhmiller, Ph.D.

7. PERFORMING ORGANIZATION NAME(S) AND ADDRESS(ES)
Jaycor
San Diego, California 92121-1190

E-Mail: jstuhmiller@jaycor.com

8. PERFORMING ORGANIZATION REPORT NUMBER

9. SPONSORING / MONITORING AGENCY NAME(S) AND ADDRESS(ES)
U.S. Army Medical Research and Materiel Command
Fort Detrick, Maryland 21702-5012

10. SPONSORING / MONITORING AGENCY REPORT NUMBER

11. SUPPLEMENTARY NOTES
Original contains color plates: All DTIC reproductions will be in black and white.

12a. DISTRIBUTION / AVAILABILITY STATEMENT
Approved for Public Release; Distribution Unlimited

12b. DISTRIBUTION CODE

13. ABSTRACT (Maximum 200 Words)

In FY04, we continued the effort to produce a methodology that estimates the probability/ severity of specific injuries from nonpenetrating, body armor impact and that can indicate the effects of body differences. We've made significant progress on the main tasks and successfully accomplished all the milestones in FY04. In summary, (1) the ATM was refined to provide more and better behind body armor impact force and motion responses; the ATM response was calibrated through laboratory drop and impact tests and validated against animal and human responses; (2) additional live fire tests were conducted to obtain better impact response measurements; clay tests were also conducted to compare the impact characteristics used in animal studies with the real behind armor impacts; (3) an addition of 9 animal tests were conducted successfully in FY04; mechanical response, anatomical, and pathological data were collected in each test; physiological measurements of SpO2, HR, were added in recent tests; pressures inside lungs were also measured in a few tests where pressure catheters were inserted into the lungs; (4) subject-specific thoracic FE models of swine subjects were refined and validated against the response measurements; excellent agreements with measured motion, impact force, and pressure wave inside lungs were obtained; (5) thoracic FE model of human were developed; (6) rib fracture and lung injury correlations were developed and validation with animal test data showed good agreement; (7) developed a numerical model of ATM which interprets the ATM measurements and determines the impact parameters to use in FE simulations; this completes the whole process of live test measurements, FE calculation of tissue responses, and BA trauma assessment.

14. SUBJECT TERMS
Behind armor injury, blunt trauma, finite element modeling

15. NUMBER OF PAGES
29

16. PRICE CODE

17. SECURITY CLASSIFICATION OF REPORT	18. SECURITY CLASSIFICATION OF THIS PAGE	19. SECURITY CLASSIFICATION OF ABSTRACT	20. LIMITATION OF ABSTRACT
Unclassified	Unclassified	Unclassified	Unlimited

FOREWORD

Opinions, interpretations, conclusions and recommendations are those of the author and are not necessarily endorsed by the U.S. Army

( ) Where copyrighted material is quoted, permission has been obtained to use such material.

( ) Where material from documents designated for limited distribution is quoted, permission has been obtained to use the material.

( ) Citations of commercial organizations and trade names in this report do not constitute an official Department of the Army endorsement or approval of the products or services of these organizations.

(x) In conducting research using animals, the investigator(s) adhered to the "Guide for the Care and Use of Laboratory Animals," prepared by the Committee on Care and Use of Laboratory Animals of the Institute of Laboratory Animal Resources, National Research Council (NIH Publication No. 86-23, Revised 1985).

( ) For the protection of human subjects, the investigator(s) have adhered to policies of applicable Federal Law 32 CFR 219 and 45 CFR 46.

( ) In conducting research utilizing recombinant DNA technology, the investigator(s) adhered to current guidelines promulgated by the National Institutes of Health.

Principal Investigator's Signature

1/6/05

Date

DAMD17-00-C-0031

Table of Contents

Page

1. INTRODUCTION **4**

2. BODY **5**

2.1 ATM IMPROVEMENT AND LIVE FIRE TESTING 5

2.1.1 Laboratory Testing of ATM 6

2.1.2 Clay and Live Fire Tests 7

2.1.3 Live Fire ATM Tests 11

2.1.4 ATM Modeling and Validation 12

2.1.5 Determination of Impact Parameters from Live Fire Test 15

2.2 ANIMAL STUDY 16

2.2.1 Test protocol and Matrix 16

2.2.2 Mechanical response 17

2.2.3 Injury data 19

2.2.4 Physiological response measurements 21

2.3 FINITE ELEMENT MODEL 21

2.3.1 Improvement of Subject-specific swine FEM 21

2.3.2 Human Thoracic FEM 23

2.4 INJURY CORRELATIONS 24

3. SUMMARY **26**

List of Figures

Page

Figure 1. Schematic of the newer version of ATM 6

Figure 2. SBA Impactor (left) and HBA Impactor (right) 8

Figure 3. Live fire clay tests (a) Clay–Armor setup; (b) Fuji film result for clay test; (c) Crater depth and diameter impact measurement 9

Figure 4. Laboratory versus Live Fire Clay Data 10

Figure 5. Live fire testing (a) ATM testing setup; (b) ATM – Armor test setup; (d) Fuji film result for ATM live fire test 11

Figure 6. Results of ATM test #5 (Armor Level IIA ; a half inch Dragonskin Cover) 12

Figure 7. Validation of FE model of ATM against drop tests 13

Figure 8. Validation of FE model of ATM against impactor on ATM tests 14

Figure 9. Validation of FE model of ATM against live fire test results 15

Figure 10. Mechanical response measurement from the May 16, 04 tests 17

Figure 11. Sample post-impact CT image shows the injuries 19

Figure 12. Major injuries observed in animal study 20

Figure 13. Comparison of skin lesion formation and ecchymoses with NATO study 20

Figure 14. Comparison of lung contusion pattern with NATO study 21

Figure 15. Subject-specific swine thoracic FE model and simulation of animal tests 22

Figure 16. Comparison of response measurements and FE predictions 22

Figure 17. Comparison of lung pressure catheter measurement and FE prediction 23

Figure 18. Human FE model 23

Figure 19. Rib fracture correlation curves based on normal and shear stresses 24

Figure 20. Comparison of constructed lung injury with FE prediction 24

Figure 21. Comparison of calculated pressure pattern and lung injury of the first test animal 25

List of Tables

Page

Table 1. Laboratory Clay Testing Results 8
Table 2. Test matrix of the live fire clay tests 9
Table 3. Live Fire Clay Test Results 10
Table 4. Test matrix of live fire ATM tests 11
Table 5. Summary of completed tests 16
Table 6. Peak Sternum Acceleration for UVA study 18
Table 7. Peak Impact Force from UVA study 19

1. Introduction

We've developed a systematic approach in the FY03 effort to produce a methodology that estimates the probability/severity of specific injuries from nonpenetrating body armor impact, and that can indicate the effects of body differences. The major components of this approach involve: (1) developing an anthropomorphically shaped impact measuring device, ATM, that properly accommodates a ballistic garment and measures the behind armor impact signatures; (2) actual measurements of the behind armor impact characteristics in live fire tests; (3) controlled animal tests, which deliver to animals a measurable load that is similar to behind armor impact, and which produce anatomical, mechanical, physiological and pathological data; (4) development and validation of subject-specific finite element models of the test subjects; (5) development and validation of human finite elements; (6) development and validation of major behind armor blunt injuries; (7) BABT trauma assessment software.

We've made significant progresse in each of the main tasks and successfully accomplished all the milestones in FY04. In summary, (1) the ATM was refined to provide more and better behind body armor impact force and motion responses; the ATM response was calibrated through laboratory drop and impact tests and validated against animal and human responses; (2) additional live fire tests were conducted to obtain better impact response measurements; clay tests were also conducted to compare the impact characteristics used in animal studies with the real behind armor impacts; (3) additionally, 9 animal tests were conducted successfully in FY04; mechanical response, anatomical, and pathological data were collected in each test; physiological measurements of SpO2, HR, were added in recent tests; pressures inside lungs were also measured in a few tests where pressure catheters were inserted into the lungs; (4) subject-specific thoracic FE models of swine subjects were refined and validated against the response measurements; excellent agreements with measured motion, impact force, and pressure wave inside lungs were obtained; (5) thoracic FE models of human were developed; (6) rib fracture and lung injury correlations were developed and validation with animal test data showed good agreements; (7) developed a numerical model of ATM that interprets the ATM measurements and determines the impact parameters to use in FE simulations; this completes the whole process of live test measurements, FE calculation of tissue responses, and BA trauma assessment

This report summarizes the objective, approach, and progress of the work in FY04.

2. Body

2.1 ATM Improvement and Live Fire Testing

An ATM prototype was improved., with the new design shown in Figure 1. The new design keeps the articulated system, as well as the anthropomorphic model frame for mounting armor vest. The sensors and backing materials, however, were significantly improved. A new material called Dragonskin rubber was used, which is known to have a similar biomechanical response as human tissue during compression. In addition to the force gauge, which is rigidly mounted on the rigid backing, the ATM also has a backing layer 6 inches in diameter and 2 inches thick embedded with 5 equally spaced accelerometer and FlexiForce sensor combination units. Each combo unit is composed of metal fixtures which have threaded inserts for accelerometer placement and a flat top face for the placement of the FlexiForce sensors. Additional backing material can be added onto ATM to achieve desired response profiles.

The force gauge, the combo units, and a high-speed camera are connected to a synchronizer and computers to collect data. The Pressurex tactile pressure measuring films (Fuji films), which measure the maximum spatial distribution, can also be placed right underneath the armor on top of the rubber.

The major advantages of the new design over the previous version includes: (1) additional impact force and motion response for better characterization of BA impact signatures; (2) more accurate measurements and less error in interpreting the measurements since the sensor units are placed directly under armor; and (3) new material that matches the human tissue better.

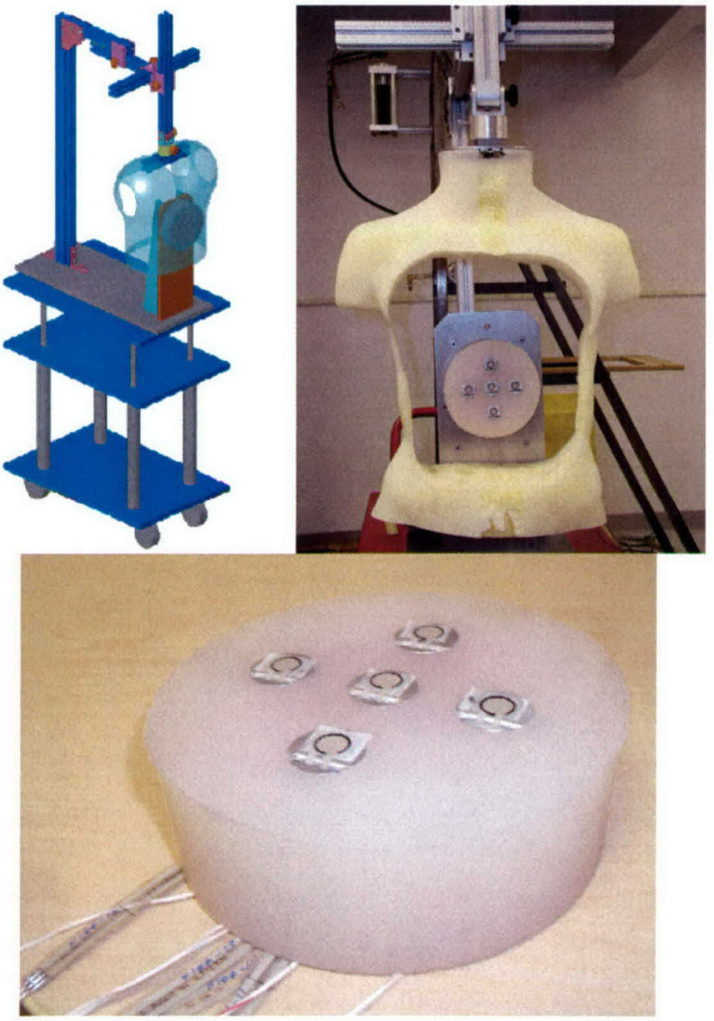

Figure 1. Schematic of the newer version of ATM

2.1.1 Laboratory Testing of ATM

Force hammer tests were conducted to determine the proper calibration of the FlexiForce sensors. This calibration was accomplished through the application of a known and measured force by a force hammer and measuring the response of the FlexiForce sensors. Each sensor was tested and calibrated individually. It was found that the conversion factors for the FlexiForce sensors all fell within a range of 7456.70 – 9594.35. The variability between individual calibration factors is closely related to the force hammer striking location in reference to the FlexiForce sensor. Those striking locations falling towards the outer edge of the sensor generally had higher calibration factors because a higher measurement was recorded from the force hammer, in comparison to the measurement read by the FlexiForce sensor. This testing provided the conversion factors for FlexiForce measurements in later data collection and analysis.

Drop tests were performed by dropping an instrumented hemispherical of known mass on the ATM protected by 1.0 inch or 0.5 inch Dragonskin coverings from a given height. This test characterized the response of ATM at low speed impacts. The acceleration time trace of the hemisphere was measured as well as the acceleration and impact force on each combo unit. Additional quantities such as velocity, deformation, force, impulse, and kinetic energy were derived from the measurements.

Impactor on ATM tests were performed by firing impactors at the ATM to characterize the response of ATM at high speed impacts. This testing was performed while covering the ATM with 1.0 and 0.5 inch Dragonskin covers, to simulate soft tissue. The impactors were shaped in such a way that the impressions and forces transmitted during the collision of the impactors and the ATM are similar to those impressions and forces observed in behind body armor impacts. Impactor velocity was measured by chronograph. High-speed movies were also recorded to capture the interaction between the impactor and the ATM.

2.1.2 Clay and Live Fire Tests

Impactor clay tests were conducted using a soft armor impactor and a hard armor impactor, as shown in Figure 2 below. These impactors have different diameter, shape and mass and simulate the behind soft and hard body armor impacts, respectively, at given speeds. Before each test, the clay was heated, using two heating pads and a reflective shell to contain the heat within the clay. The average temperature, taken along four equally spaced depths at nine equally spaced locations on the clay surface, was 93°F. During the tests, the impactors were driven by a piston that was launched by high pressure helium gas. The pressures in the tests varied from 100-800psi. These impactors free-flew after the launching rod was pushed to the end of its length, culminating in the collision with the clay block. The results from the clay tests performed using the impactors are given in Table 1.

Figure 2. SBA Impactor (left) and HBA Impactor (right)

Table 1. Laboratory Clay Testing Results

Impactor Type	Pressure (psi)	Mass (g)	Crater Depth (mm)	Crater Radius (mm)	Crater Volume (cm)^3
SBA-45	100	0.053	15.0	23.5	10.4
SBA-45	200	0.053	21.5	29.0	22.7
SBA-45	300	0.053	29.0	34.0	42.1
SBA-45	400	0.053	34.8	37.5	61.4
SBA-45	500	0.053	39.0	38.5	72.6
SBA-45	800	0.053	45.5	40.0	91.4
SBA-15	100	0.05	12.0	31.0	14.5
SBA-15	200	0.05	17.0	31.5	21.2
SBA-15	300	0.05	21.5	35.0	33.1
SBA-15	400	0.05	26.0	39.0	49.7
SBA-15	500	0.05	28.5	39.5	55.9
SBA-15	800	0.05	33.0	43.8	79.3

Additional **live fire clay tests** were conducted on both ATM and clay backing material. In the clay tests, soft body armor (SBA) of varying levels were placed over a pre-heated and preconditioned clay block (Figure 4.1a). Fuji film was placed between the clay and the armor to help ascertain the exact location of the impact and the relative shape of the crater behind the armor after impact (Figure 4.1b). Following the test, crater depths and diameters were recorded for later analysis (Figure 4.1c). The level of armors, bullet types and speeds are given in Table 2.

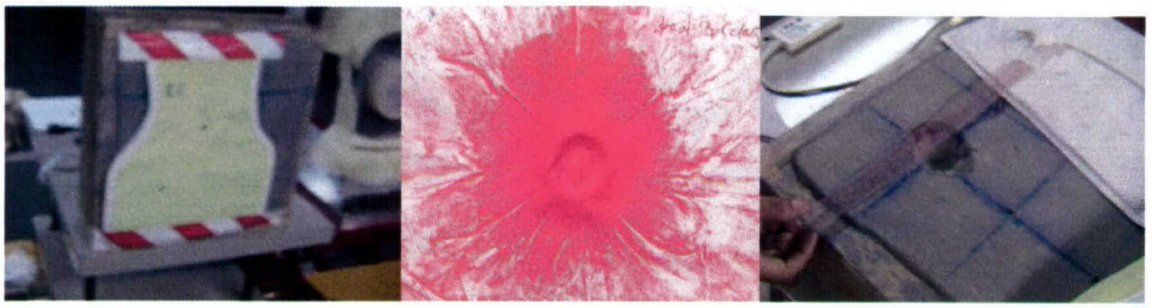

Figure 3. Live fire clay tests (a) Clay–Armor setup; (b) Fuji film result for clay test; (c) Crater depth and diameter impact measurement

Table 2. Test matrix of the live fire clay tests

Test #	SBA Level	Cartridge	Expected Velocity (ft/s)
0	IIA	124gr Federal Hydra-Shok HP	1120
1	IIA	124gr Federal Hydra-Shok HP	1120
2	II	124gr Federal Hydra-Shok HP	1120
3	IIIA	115gr Corbon JHP	1350

The results from the live fire tests performed on the clay are given in Table 3. These results were analyzed and then compared against the results from the laboratory clay test, as a means to validate the ability of the impactors to produce craters of similar dimensions to those observed in live fire testing. Figure 4 shows that the crater from the 45 degree smaller impactor matched very close to the live fire test results, indicating that it was a good simulator of behind body armor impacts at the velocity range used in the tests.

Table 3: Live Fire Clay Test Results

Test #	SBA Level	Cartridge Type	Depth (mm)	Radius 1 (mm)	Radius 2 (mm)	Volume (cm^3)
0	IIA	124gr Federal Hydra-Shok HP	32	28.6	38.1	43.8
1	IIA	124gr Federal Hydra-Shok HP	32	28.6	38.1	43.8
2	II	124gr Federal Hydra-Shok HP	23	31.8	38.1	35.0
3	IIIA	115gr Corbon JHP	26	31.8	34.9	36.2

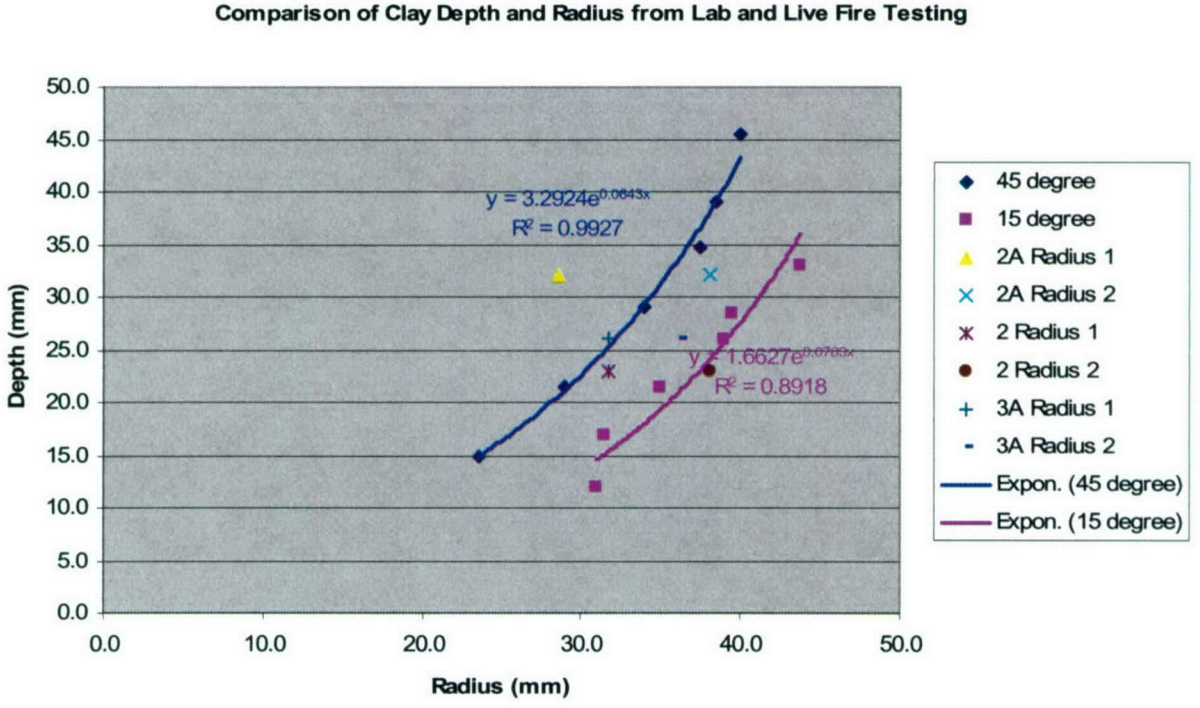

Figure 4. Laboratory versus Live Fire Clay Data

2.1.3 *Live Fire ATM Tests*

For live fire ATM tests, varying thicknesses of Dragonskin, half inch and one inch, were then placed on top of ATM to both protect the sensor units and to simulate the soft tissue covering the thorax. SBA of varying levels were placed over the thorax, with Fuji film placed between the Dragonskin surface and the SBA (Figures 4.2b). Accelerometers, FlexiForce sensors, chronographs, and a high speed camera were used to record loading measurements, bullet velocities, and wave propagation along the armor surface during each live fire test. The level of armors, bullet types and speeds are given in Table 4

Figure 5. Live fire testing (a) ATM testing setup; (b) ATM – Armor test setup; (d) Fuji film result for ATM live fire test

Table 4: Test matrix of live fire ATM tests

Test #	SBA Level	Cartridge	Expected Velocity (ft/s)	Cover Thickness
4	II	124gr Federal Hydra-Shok HP	1120	1.0"
5	IIA	124gr Federal Hydra-Shok HP	1120	1.0"
6	IIIA	115gr Corbon JHP	1350	1.0"
7	II	124gr Federal Hydra-Shok HP	1120	0.5"
8	IIA	124gr Federal Hydra-Shok HP	1120	0.5"
9	IIIA	115gr Corbon JHP	1350	0.5"

The measurements in all the tests were successful. Sample results for ATM test 5 are given in Figure 6. In this specific test, a half inch Dragonskin rubber layer was placed on top of the measuring layer and the bullet struck on the armor right above the location of the center sensor units. Both the acceleration and force at the center unit were significantly higher that the other units. The measurements from accelerometer and the Flexiforce appeared to be synchronous. Further analysis of data indicated that the center unit reached a velocity of more than 20m/s in less than a quarter of a millisecond. The peak deformation was about 2 cm, occurring at about 1.5 milliseconds. The impulse and work transferred to the ATM concentrated around the center unit.

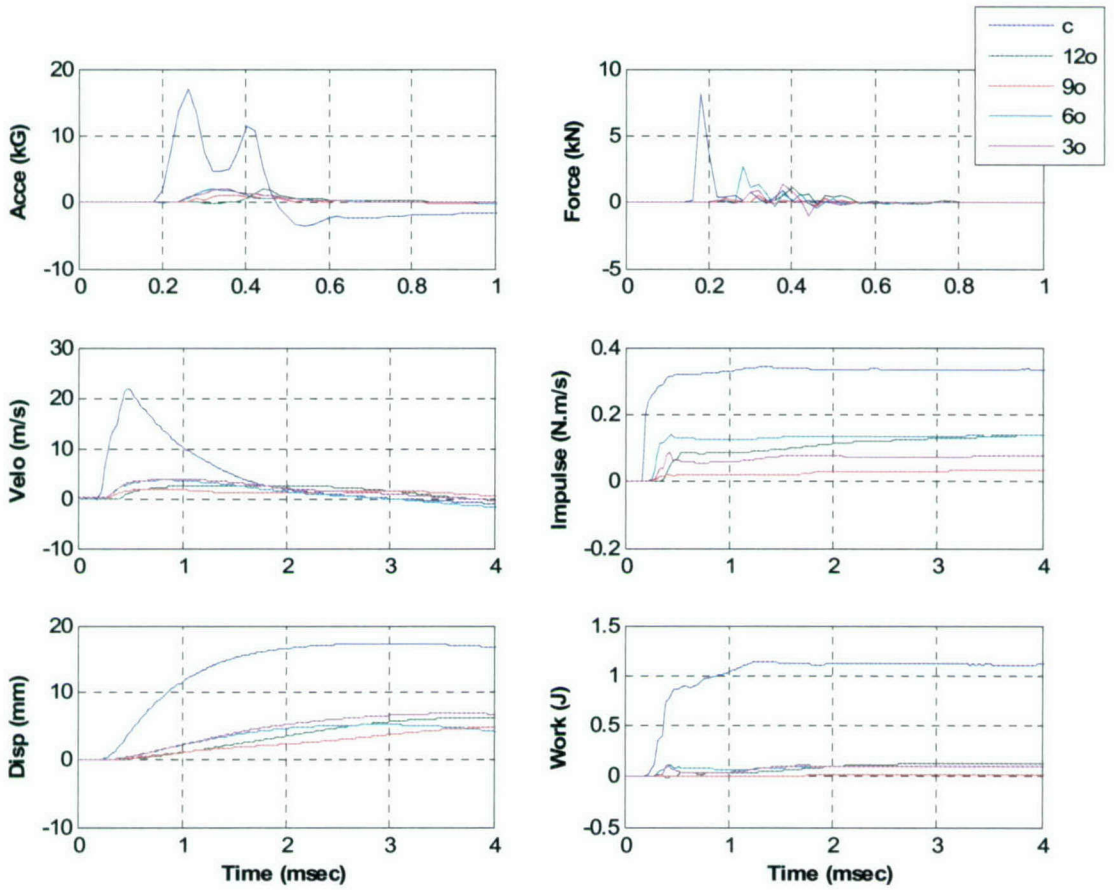

Figure 6. Results of ATM test #5 (Armor Level IIA ; a half inch Dragonskin Cover)

2.1.4 ATM Modeling and Validation

For interpreting ATM measurements and calibrating the response characteristics of ATM, finite element models were developed for the ATM and were validated against the drop

tests and impactor on ATM test data. FE simulations and the comparison of the calculated motion results were given in Figure 7 and Figure 10 respectively. These results indicated that the ATM FEM accurately predicts the ATM responses.

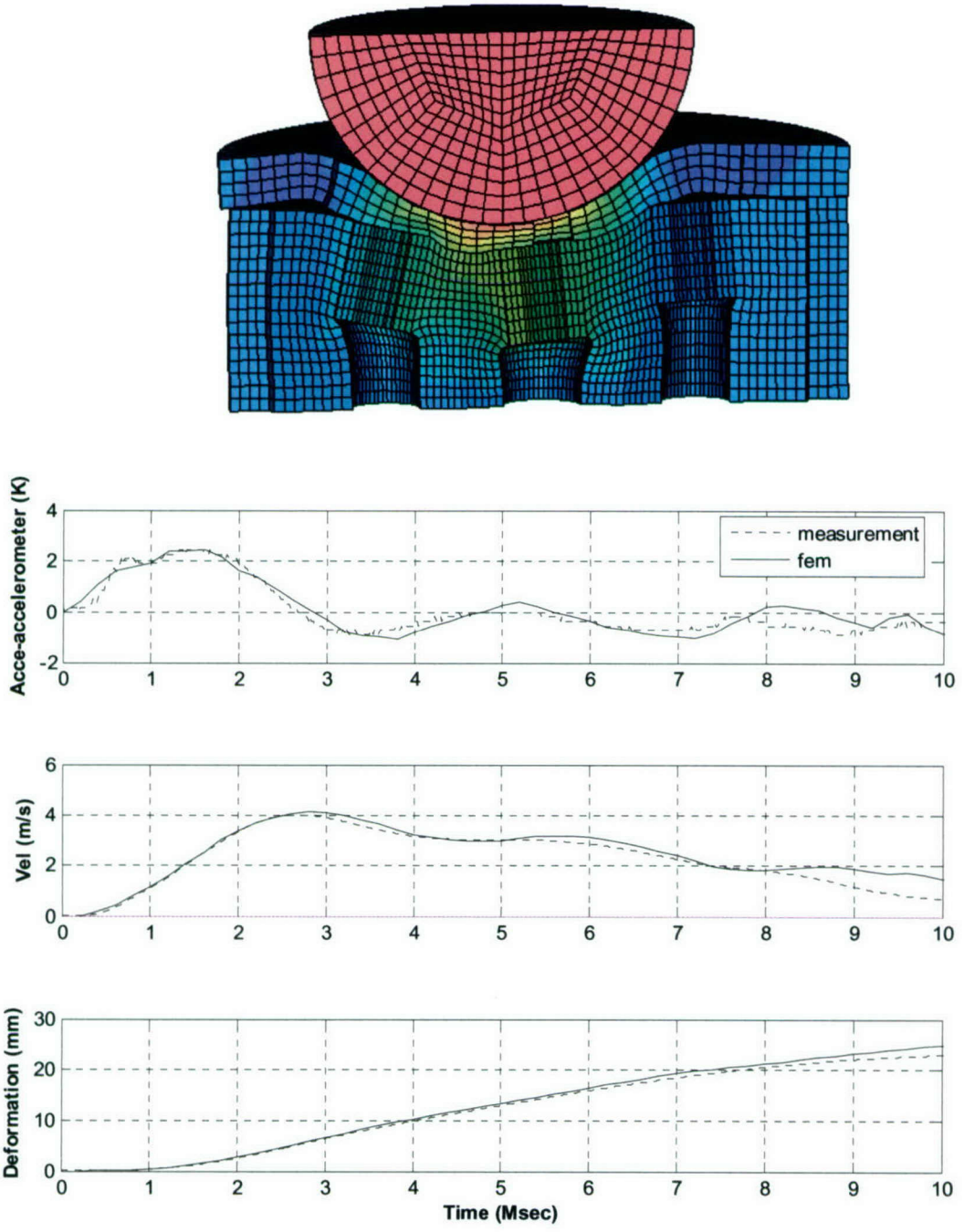

Figure 7. Validation of FE model of ATM against drop tests

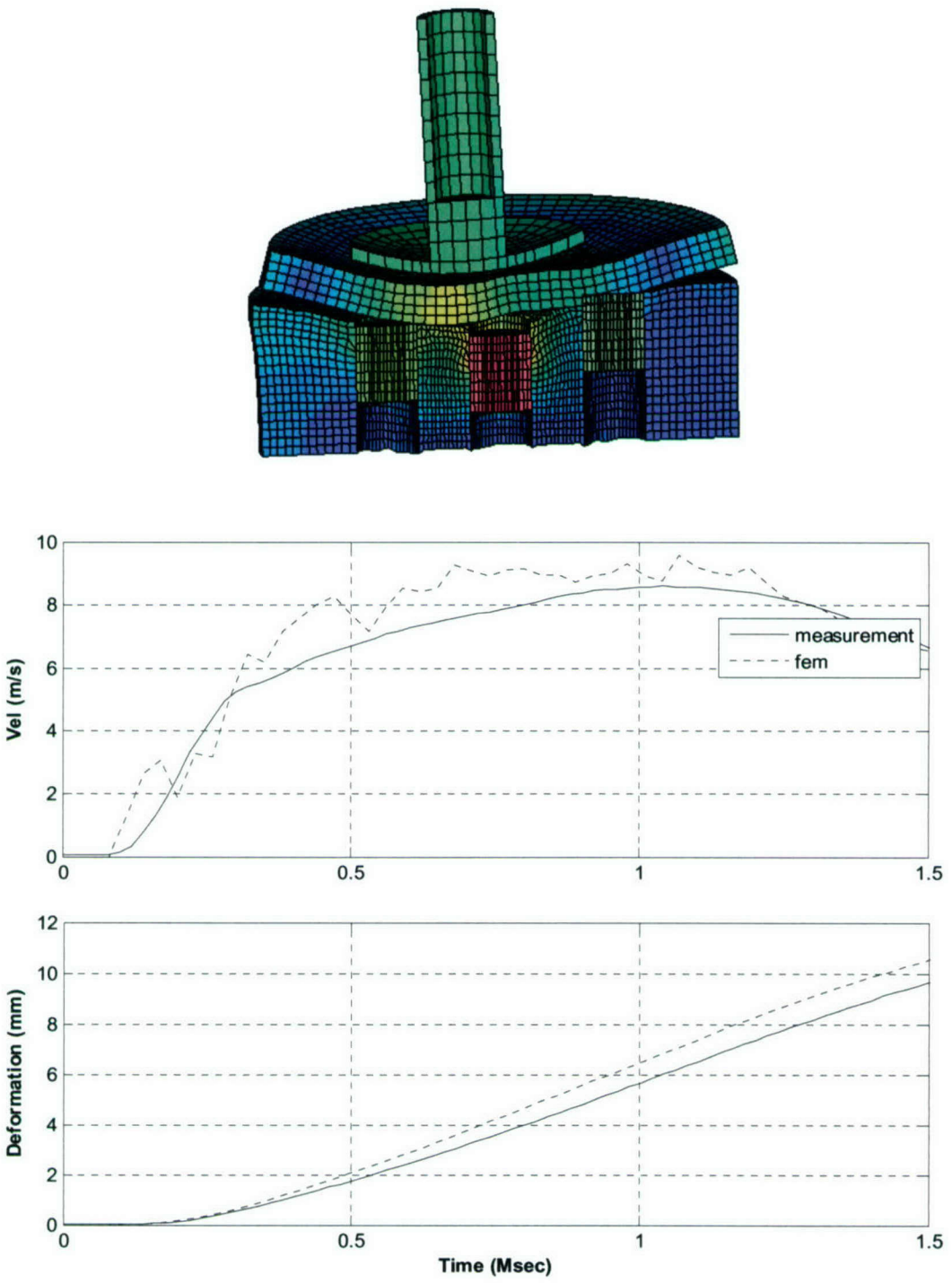

Figure 8. Validation of FE model of ATM against impactor on ATM tests

2.1.5 *Determination of Impact Parameters from Live Fire Test*

The validated FE model of ATM was then used to determine effective behind armor impact. To accomplish this, FE models of a bullet and a material layer that simulates the body armor were introduced. The armor simulating layer was modeled as a simple material which involves several material parameters, reflecting the overall armor response during the impact. Inverse solution of the problem by iteration determines the parameters that best match the ATM measurements. A comparison of simulation and live fire test results is given in Figure 9.

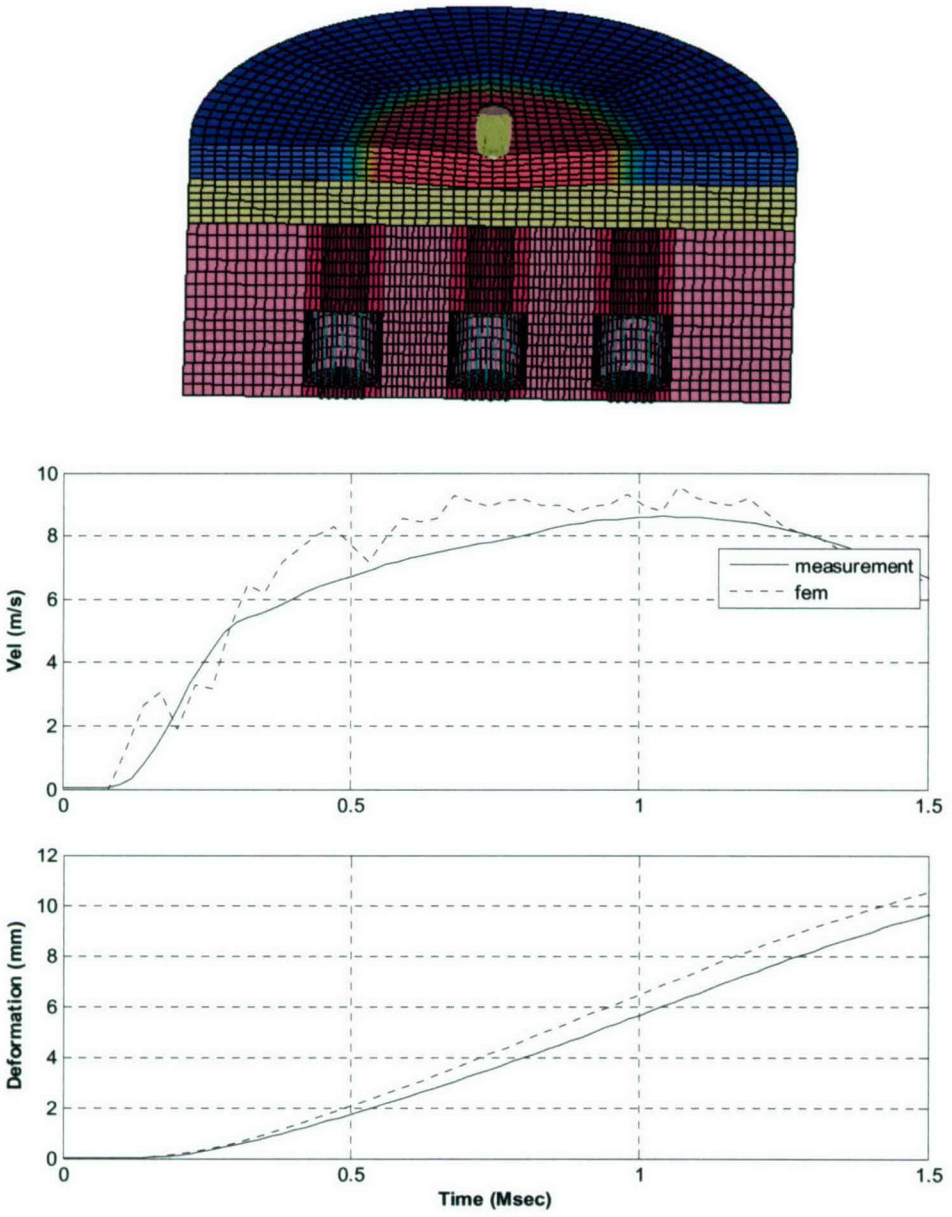

Figure 9. Validation of FE model of ATM against live fire test results

2.2 Animal Study

2.2.1 *Test protocol and Matrix*

An animal protocol was developed in cooperation with the researchers at the University of California at San Diego (UCSD) in FY03. This protocol was renewed in FY04. The actual protocol is as follows. Pigs will be anesthetized in the UCSD/CTF laboratory, intubated (6.0-8.0 ID oral-nasal tube with inflation cuff), and a venous catheter secured in the groin for contrast administration. Animals will be kept warm using a water-controlled heating pad except during transport. An ultrasound study of the liver and spleen will be performed with ultrasound contrast. They will be transported to the CT suite (200 yards away), imaged with CT with intravenous contrast (1ml/kg), transported back to the laboratory and one impact test will be conducted. The animals are then transported back to the CT suite and reimaged with a second dose of 1ml/kg IV contrast. They will finally be euthanized and necropsied to assess the chest wall and internal organs for injury. Anatomical data (weight, size, critical dimensions) will be collected for each animal.

A total of 12 tests have been completed successfully, among which 9 were completed in FY04. The test matrix and parameters were given in the following Table 5.

Table 5. Summary of completed tests

Test Date	Impactor Type	Mass (kg)	Peak Impact Acceleration (kG)	Impact Velocity (m/s)
02/02/03	15° L	0.075	21.99	25.88*
03/22/03	15° L	0.075	21.58	35.78**
05/23/03	15° L	0.075	17.78	35.52
12/06/03	15° L	0.075	15.84	35.85
01/24/04	15° L	0.075	9.14	37.72
02/28/04	15° L	0.075	17.47	38.71
03/13/04	15° L	0.075	17.43	39.69
04/09/04	15° L	0.075	18.96	41.92
05/16/04	15° L	0.075	22.37	42.75
06/05/04	15° L	0.075	12.92	35.99
07/17/04	15° L	0.075	9.95	42.30
08/21/04	45° Sm	0.053	12.61	46.13

2.2.2 *Mechanical response*

The impactor used in the animal tests was instrumented with a high-shock accelerometer. The impact acceleration was measured, and the impact velocity, deformation, and force time histories were derived from the data. A sample result of one of the tests is given in Figure 10. It shows that the peak impact acceleration is around 20kG. The peak deformation is around 18 mm, occurring about 1.5 milliseconds after the impact. The peak impact force is about 15 kN.

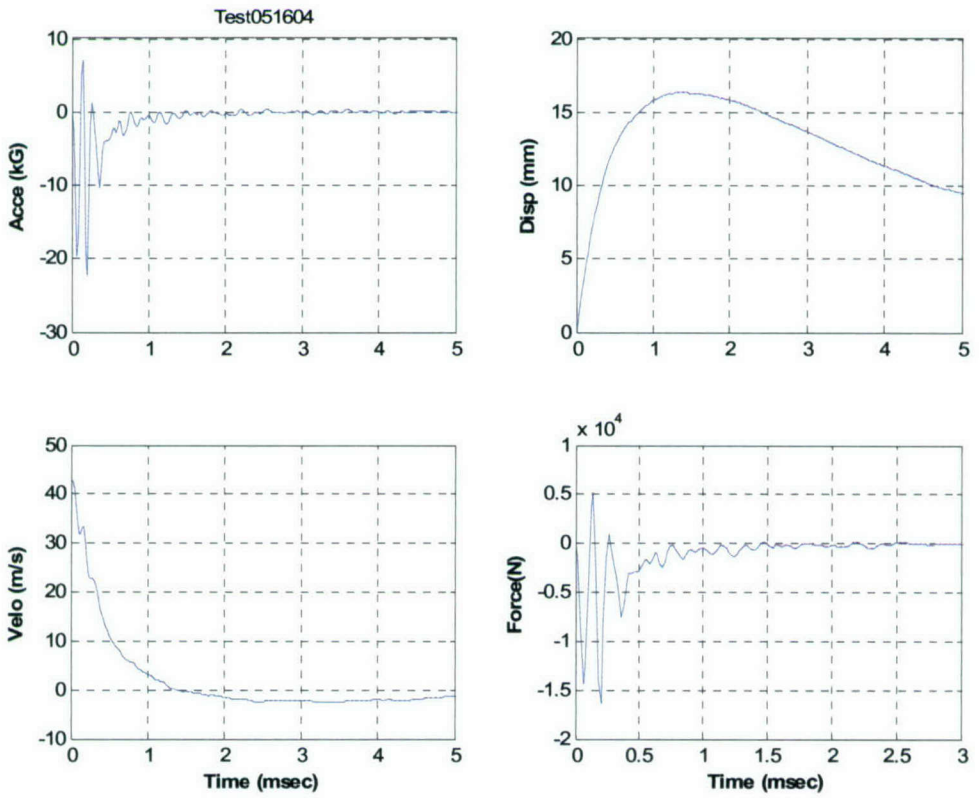

Figure 10. Mechanical response measurement from the May 16, 04 tests

The mechanical response measurements obtained from the animal tests were compared against the measurements from the NATO-Oksbol tests. The NATO test used 27 animals, which were randomly assigned to one of four groups The animals were protected by three armor configurations and shot by 7.62 mm NATO bullets fired from a fixed barrel mounting. One accelerometer and one pressure gauge were mounted on one rib of each animal near the impact location.

The analysis, however, indicates that the pressure and acceleration time traces from the NATO tests are highly noisy, and the peaks for each vary significantly. In addition, negative acceleration time traces are observed in the NATO data. It was most likely due to mounting the sensors to a non-rigid surface. Thus, alignment problems could occur with a negative bending motion being recorded by the accelerometer.

The peak impactor velocities from the animal tests primarily ranged from 35-50 m/s and resulted the peak rib velocity between 20-35 m/s from our FE simulations. The NATO tests yielded lower rib velocities ranging from 10-25 m/s. The lower values from NATO tests could be due to several reasons, including testing setup, firing angle, or sensor configuration. As was already stated, the accelerometer time traces for the NATO study were faulty, and thus the velocity time traces used to calculate impact velocity from them were faulty, as well. However, their values did indicate that our controlled animal test did deliver an impact loading that was compatible to real behind armor loading.

The animal response data were also compared with the measures from the cadaver tests conducted by Bass et al. In those tests, cadaver specimens were protected by ballistic material and hard armor plate and were impacted on the thorax. The report from Bass et al., however, did not provide any information concerning individual cadaver responses. Instead, peak sternum acceleration and peak impact force are plotted against muzzle velocity for the various specimens. However, comparison of the peak acceleration and peak impact force show that that the cadaver measurements appeared to be in very close range with the measurements obtained from our animal test. This also suggests that the impact parameters we used match the real behind armor impact loading.

Table 6: Peak Sternum Acceleration for UVA study

Data Point #	Peak Sternum Acceleration (kG)
1	19.0
2	38.0
3	25.0
4	13.0
5	120.0
6	9.0

Table 7: Peak Impact Force from UVA study

Data Point #	Peak Impact Force (kN)
1	15.0
2	24.0
3	28.0
4	27.5
5	25.5
6	24.0
7	18.5
8	18.0

The animal protocol was also modified in FY04 to allow us to inset a few pressure catheters into the lungs of the animal test subjects. Three tests with pressure catheters have been completed, with excellent measurements of lung pressures at different locations ranging from directly underneath the impact spot, to about 15 cm away from the impact, to the other side of lungs. The measurements were successful and the analysis of data is being conducted.

2.2.3 Injury data

A post-impact CT image is given in the following Figure 11, indicating the success of using post-impact imaging in quantifying behind armor trauma.

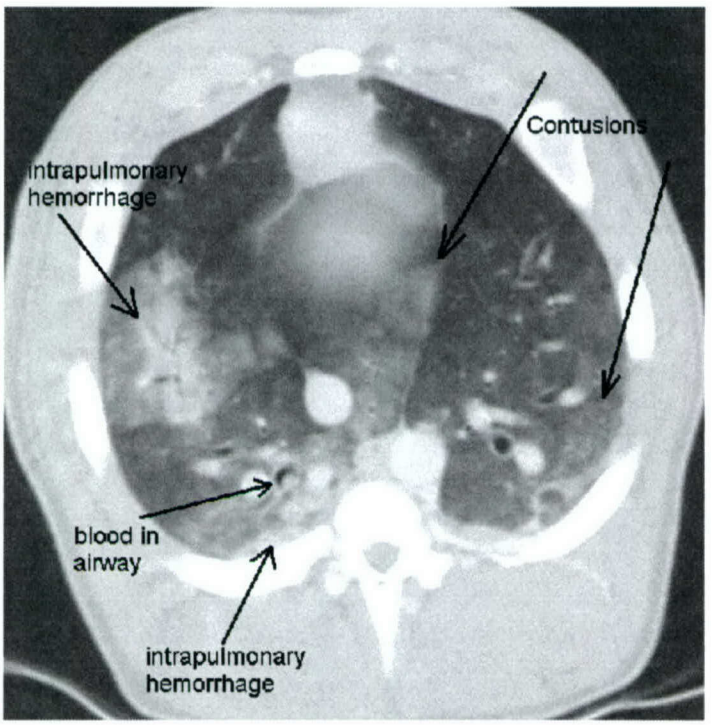

Figure 11. Sample post-impact CT image shows the injuries

Necropsy studies showed that fractured ribs and lung contusions were the major injuries resulting from testing. Several tests impacted the lower thorax of the animal and resulted in lung contusion, liver laceration, rib fractures, and mild heart lesion. Figure 12 shows pictures of observed major injuries.

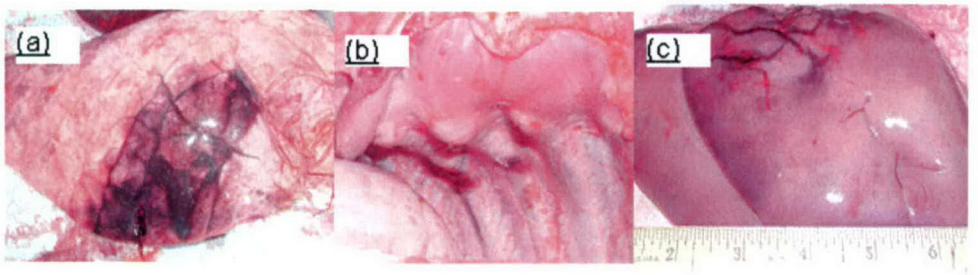

Figure 12. Major injuries observed in animal study

The injuries sustained by the subjects in the animal study compared well, and exhibited similar tendencies, when contrasted against the injury patterns in other experiments. The impacts from the animal study caused bruising and skin lesions to immediately form following the intervention. As time progressed, ecchymotic areas began forming in a similar manner to that observed in the NATO and the Magnan and Sarron studies (see Figure 13 below).

Figure 13. Comparison of skin lesion formation and ecchymoses with NATO study

Rib fractures were another representative injury observed in the animal tests, occurring at least once in 65% of the specimens tested. In 50% of the specimens tested, there were multiple rib fractures. Once again, these injuries were a dominant feature of the injury patterns observed in the other experiments.

Just as the NATO and the Magnan and Sarron studies had pulmonary contusions form on test specimen lungs, pulmonary contusions existed on 94% of all JayPig specimens tested. These primarily occurred on the impact side of the lungs, although 44% had contusions and

damage existing on both left and right lungs. Examples of these damaged lungs can be viewed in Figure 14.

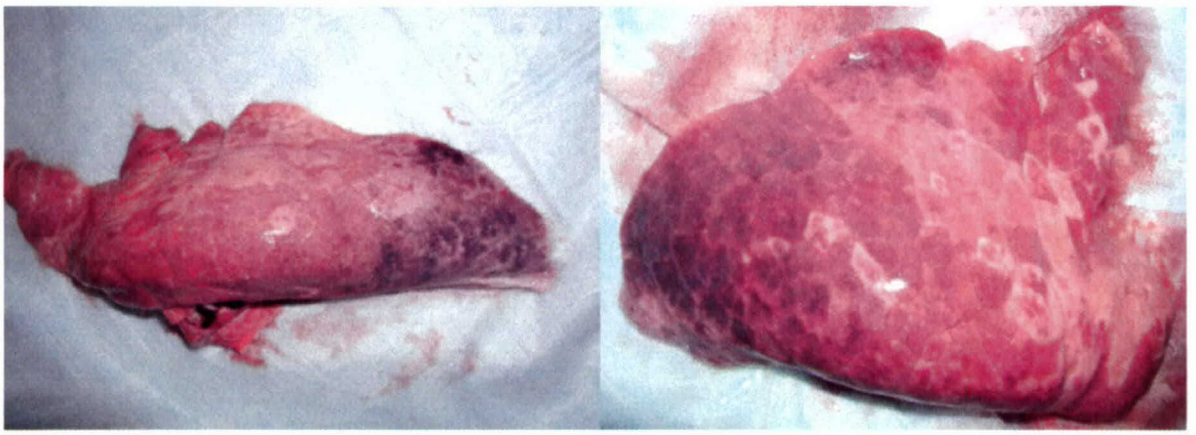

Figure 14. Comparison of lung contusion pattern with NATO study

2.2.4 *Physiological response measurements*

The measurements of heart rate (HR) and oxygen saturation (SpO2) were also added into our animal protocol during the FY04. The collected data is being analyzed.

2.3 Finite Element Model

2.3.1 *Improvement of Subject-specific swine FEM*

A method for developing swine thoracic FEM, based on CT images of a specific animal subject, was developed in FY03. FY04 efforts focused on the improvement of the model and validation of the model against test measurements. The major improvements made in this year include: better ribcage–lung interface treatment; addition of lung pleural surface; better treatment of rib contract; and better muscle and skin material parameters, which are calibrated from the test measurements. The improved model is shown in Figure 15. The improved models were validated against the test measurements. Excellent agreements were achieved as shown in Figure 16 and Figure 17.

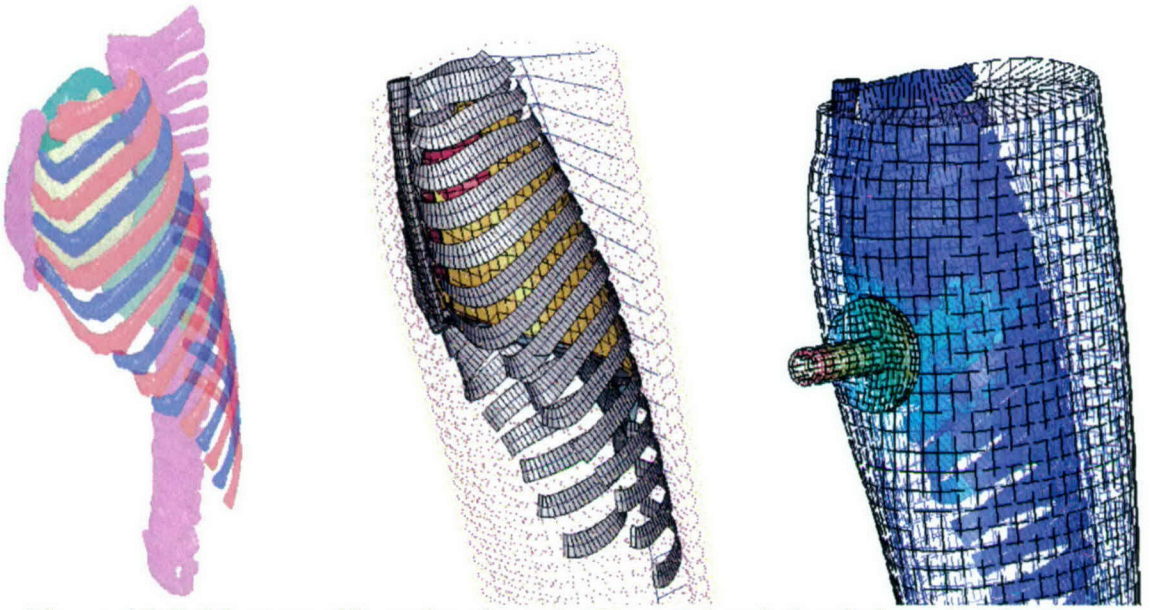

Figure 15. Subject-specific swine thoracic FE model and simulation of animal tests

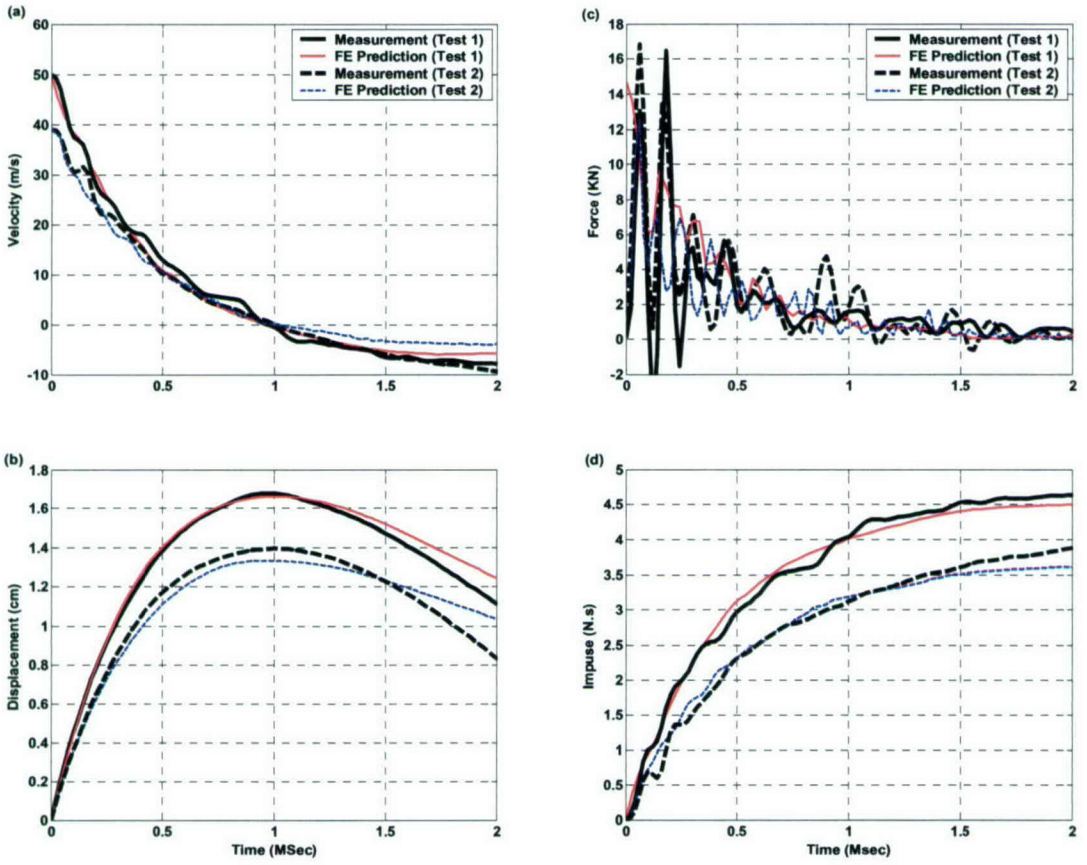

Figure 16. Comparison of response measurements and FE predictions

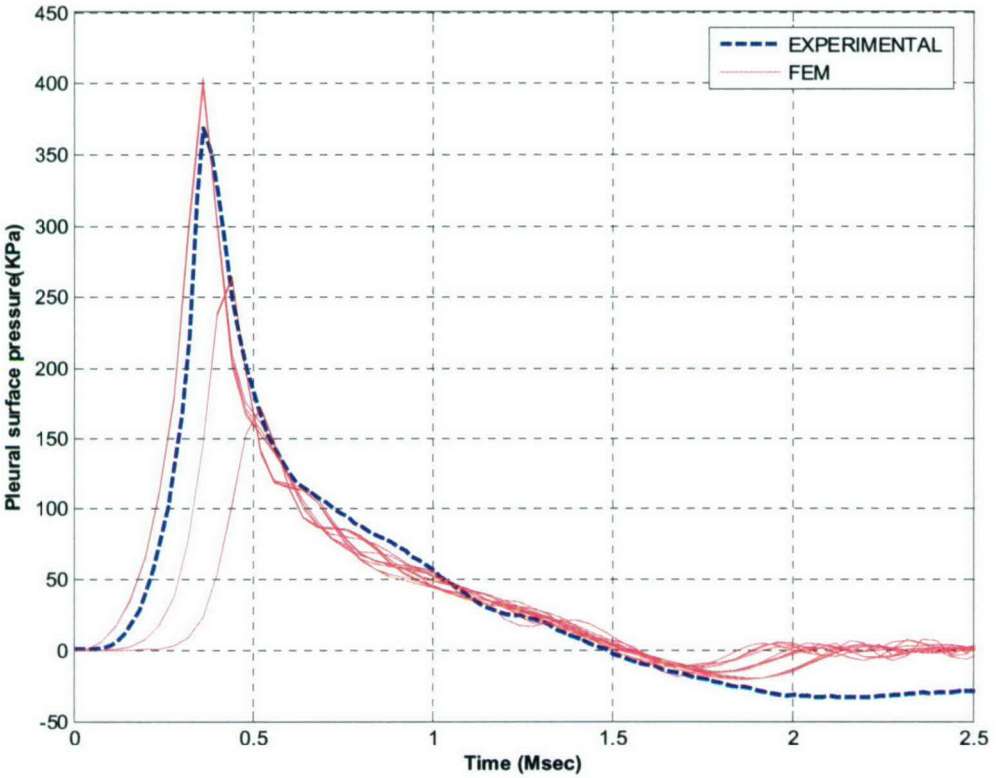

Figure 17. Comparison of lung pressure catheter measurement and FE prediction

2.3.2 *Human Thoracic FEM*

A Human FE model, based on the Visible Man data set, was also developed and used in blunt impact simulation, as shown in Figure 18.

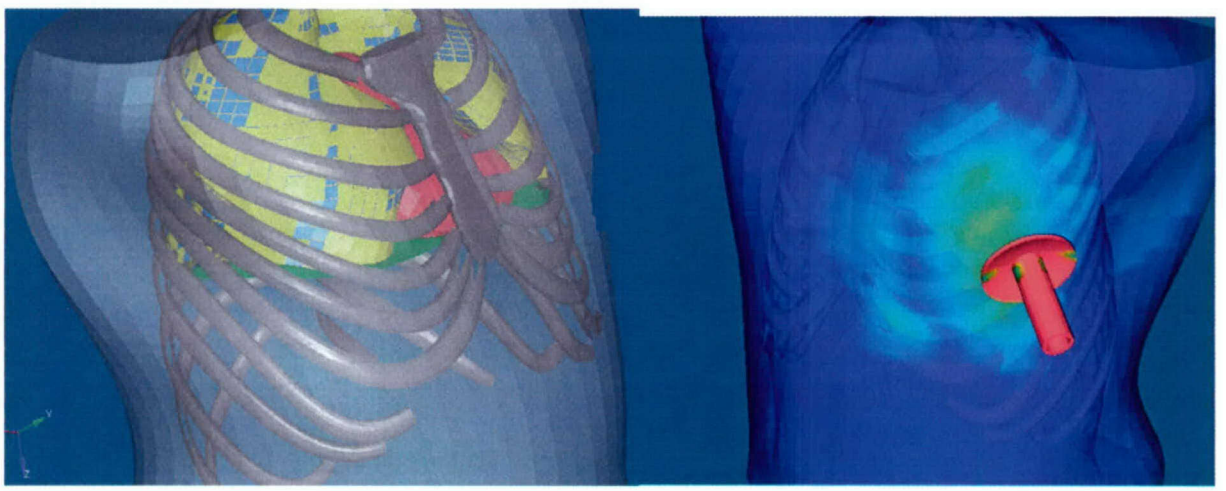

Figure 18. Human FE model

2.4 Injury Correlations

Injury correlations, using maximum stress as a predictor, were developed for predicting rib fracture, based on the FE simulations and animal test results. The regression curves are given in Figure 19.

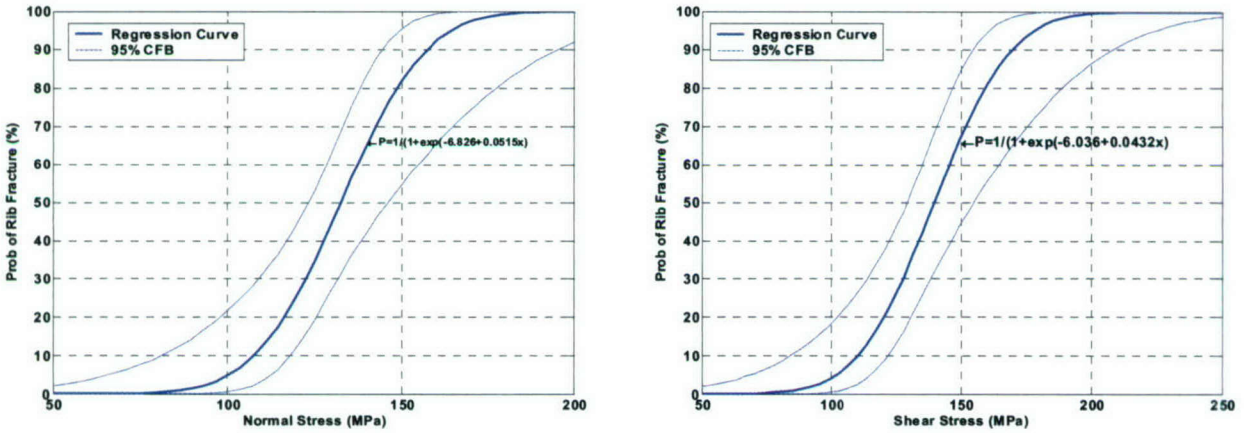

Figure 19. Rib fracture correlation curves based on normal and shear stresses

For lung contusion prediction, the formulation of normalized work was modified, and energy density was adopted as the predictor of lung injury at a local scale. Figure 20 compares the actual contusion, constructed from post-impact CT images with the prediction from FE simulation. The comparison of FE prediction with necropsy data is given in Figure 21.

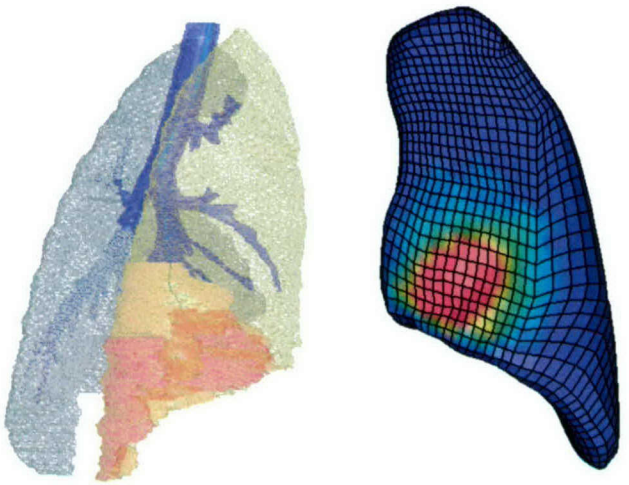

Figure 20. Comparison of constructed lung injury with FE prediction

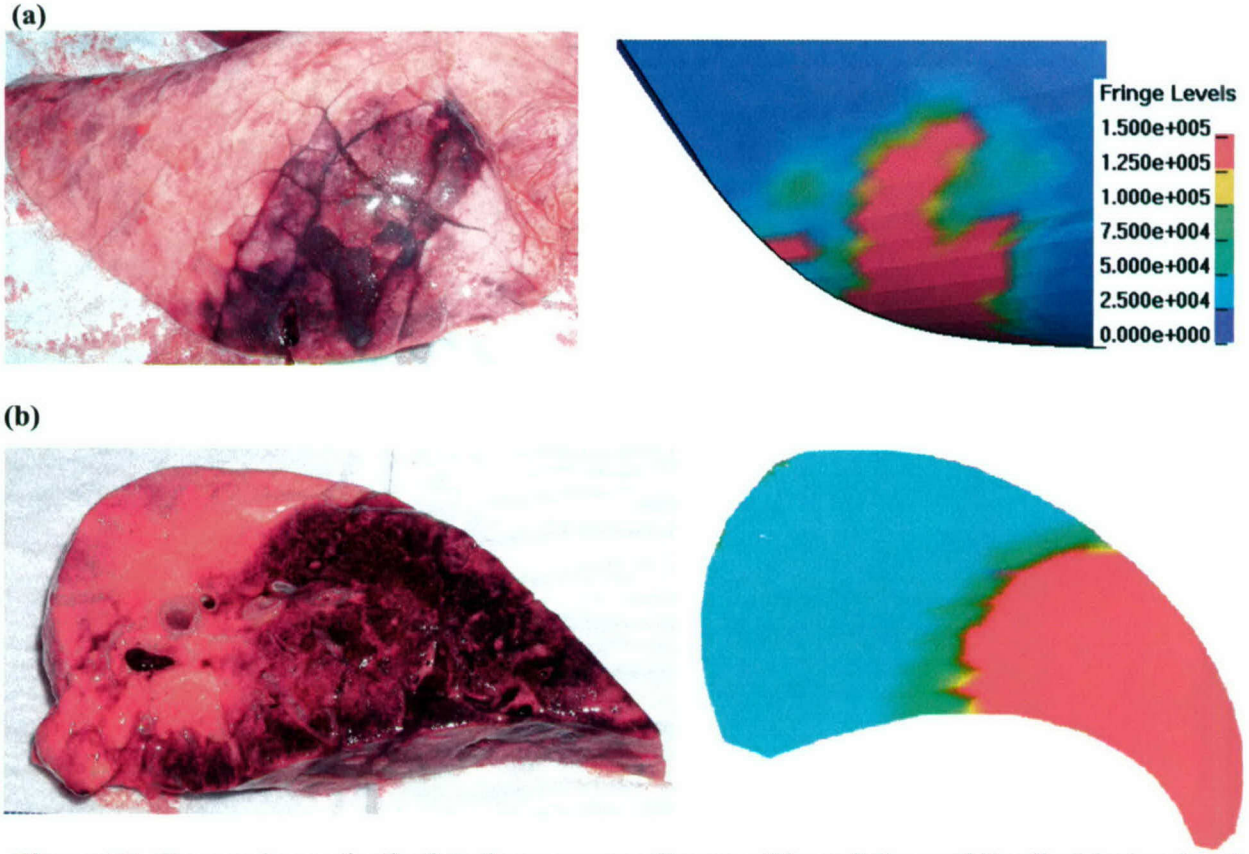

Figure 21. Comparison of calculated pressure pattern and lung injury of the first test animal

(a) Injury and pressure on pleural surface; (b) Injury and pressure inside the lung

3. Summary

In summary, we made significant progresses in the main tasks of the projectile and successfully accomplished all the milestones in FY04.

1. We improved the ATM design, constructing a new ATM which used new backing material and added in additional measurements close to the ATM-armor interface. The new design has significant advantages over the previous version including: (1) additional impact force and motion response for better characterization of BA impact signatures; (2) more accurate measurements and less error in interpreting the measurements, since the sensor units are placed directly under armor; and (3) new material that matches the human tissue better.
2. We conducted a series of laboratory test, including drop tests and impact tests to calibrate and validate the response of the ATM.
3. We conducted impactor on clay tests, live fire clay tests, and live fire ATM tests. Analysis of test results indicated that the impactor we used in the laboratory and animal tests closely match the ballistic behind armor signature. ATM also performed well during the live fire tests and provided good and reliable measurements.
4. We conducted 9 additional animal tests in FY04. In addition to the response, anatomical, and pathological data, key physiological measurements such as SpO2 and HR were included. We also successfully obtained the modification of existing protocol to allow the insertion of pressure catheter into animal lungs. Several tests were conducted successfully to measure the pressure wave propagation inside the lung.
5. We further improved the swine thoracic FE model and validated the model against the test measurements. Excellent agreements were achieved for the mechanical response and lung pressure traces.
6. A Human thoracic FE model was developed, based on the Visible Man data set.
7. Based on the animal test data and some historical data, we developed a stress-based rib fracture criterion. Energy density, which was modified from normalized work to account for the factor that injury occurs at a local scale, was used as the predictor of lung contusion.
8. The FE model of ATM was developed and validated against the drop tests, impactor on ATM tests, and live fire tests. This model will be integrated into the behind armor blunt trauma assessment software and will determine the key impact parameters from the measurements of the ATM.